JOURNAL OF MOLECULAR SPECTROSCOPY **174,** 365–378 (1995)

The CN Mode of HCN: A Comparative Study of the Variation of the Transition Dipole and Herman–Wallis Constants for Seven Isotopomers and the Influence of Vibration–Rotation Interaction

ARTHUR MAKI,* WOLFGANG QUAPP,† STEFAN KLEE,‡
GEORG CH. MELLAU,‡ AND SIEGHARD ALBERT‡

**15012 24 Avenue S.E., Mill Creek, Washington 98012-5718; †Mathematisches Institut, Universität Leipzig, Augustus-Platz 10-11, D-04109 Leipzig, Germany; and ‡Physikalisch-Chemisches Institut, Justus-Liebig-Universität Giessen, Heinrich-Buff-Ring 58, D-35392 Giessen, Germany*

Received July 19, 1995; in revised form September 5, 1995

The electric dipole transition moments and vibration-rotation constants of the CN stretching bands of $H^{12}C^{14}N$ and six other isotopomers are reported. Hot-band measurements show the vibrational dependence of the constants. Infrared absorption spectra were measured with a Fourier transform interferometer and a multipass absorption cell with a path length of up to 240 m. The transition wavenumber measurements were used to derive vibration–rotation constants, and the intensities of individual lines were used to determine the transition dipoles and Herman–Wallis factors. The unusually small transition dipole coupled with the large dipole moment of HCN (2.98 D) results in very large values for the first Herman–Wallis factor A_1 and distorts the shape of the intensity envelope of the band. These measurements show how changes in the masses of the heavy atoms in the molecule have a systematic effect on the transition dipole and on the intensity pattern of the CN stretching band.

INTRODUCTION

The CN fundamental vibrational mode of hydrogen cyanide (HCN) at 2097 cm^{-1} is a notoriously weak absorption band with a curious gap in the intensity of the rotational transitions of the *R* branch near *R*(7). The gap or intensity minimum is shifted to *R*(4) in $HC^{15}N$, *R*(1) in $H^{13}CN$, and it jumps to $J = 1$ in the *P* branch, *P*(1), in $H^{13}C^{15}N$. A similar behavior is shown by the hot-band transitions, 01^11-01^10, except that the gap is in the *P* branch for those cases that have been observed. We have measured these effects and give a quantitative explanation using the theory of line intensities with the inclusion of vibration–rotation interaction as described by Jacobi and Jaffe (*1*) and later by Watson (*2*). Note that in this paper we designate the CN stretching vibration as ν_3 and the CH stretch as ν_1.

We present here a study of the intensity of the rotational lines of the spectrum of the CN stretching region from 1850 to 2200 cm^{-1} for $H^{12}C^{14}N$ and six other isotopomers, $H^{13}C^{14}N$, $H^{12}C^{15}N$, $H^{13}C^{15}N$, $D^{12}C^{14}N$, $D^{13}C^{14}N$, and $D^{12}C^{15}N$. The first hot band also has been measured for six of these isotopomers. This is the third paper reporting the results of extensive infrared measurements that we have made on HCN (*3, 4*). Other papers will report the results of wavenumber and intensity measurements of other bands of HCN and its different isotopomers.

Low-resolution intensity measurements of these bands were first made by Hyde and Hornig (*5*). Through their analysis of the intensity of all three fundamental bands of HCN and DCN, they showed that the low intensity of the so-called CN stretching

0022-2852/95 $12.00

vibration of HCN is due to a near cancellation of contributions from the CH and CN stretching motions. If the so-called CN stretching vibration only involved a stretching of the C—N bond, the vibrational frequency would be the same for $H^{13}CN$ and $D^{12}CN$. More recent analyses by Bruns and Pearson (*6*), by Bruns and Neto (*7*), and by Kim and King (*8*) refine, but do not change this picture.

Since the transition moment for the CN stretching fundamental of HCN is a small number that results from the near cancellation of two larger numbers, any small change in the values of the large numbers, such as might result from a change in the mass of the heavy atoms, will likely cause a large change in the difference. This work was initiated in part to study this heavy atom mass effect on the intensity of the CN fundamental.

In a diatomic molecule, the case originally studied by Herman and Wallis (*9*), there is a centrifugal-distortion-like term that couples the dipole moment of the molecule with the transition dipole for vibration. If the dipole moment happens to be large and the transition dipole is small, then even a weak coupling may result in a significant change in the resultant effective transition dipole as one goes to higher rotational transitions. Herman and Wallis showed that the intensity perturbation is characterized by an enhanced intensity in either the *P* or *R* branch, depending on the relative signs of the dipole moment and the transition dipole, and a diminished intensity in the other branch. For diatomic molecules the theory was worked out in subsequent papers of those authors and others (*10–14*).

The application to triatomic molecules has been treated by Jacobi and Jaffe (*1*) and more recently by Watson and Aliev (see (*2*, *15–17*)). Jacobi and Jaffe showed that one consequence of the small transition moment of the CN stretch of HCN will be a large Herman–Wallis constant. A similar intensity effect has been measured by Arcas *et al.* (*18*, *19*) for the $[11^10, 03^10]_{I,II}-00^00$ bands of CO_2.

Earlier high-resolution measurements have been made for the 2000 cm^{-1} region by Maki and Lide (*20*), by Maki and Sams (*21*), and by Choe *et al.* (*22*). Those papers only presented wavenumber measurements and did not address the intensity problem, although the unusual pattern of intensities was recognized.

Because the Raman effect depends on the polarizability properties of the molecule rather than the dipole moment change, the rovibrational Raman spectrum of the CN stretching fundamental of HCN does not show this anomalous intensity pattern (*23*).

EXPERIMENTAL DETAILS

The spectra used in the present analysis were recorded on a Fourier transform spectrometer in the region from 1800 to 2250 cm^{-1}. The unapodized instrumental resolution was between 0.0024 and 0.0037 cm^{-1}, smaller than the Doppler width of HCN at room temperature (0.005 cm^{-1}). The measurements were made on the Bruker IFS120HR interferometer in the Giessen laboratory which has vacuum transfer optics and various absorption cells including a stainless steel White-type multipass cell with a base length of 4 m (*24*). The measurements of the heavy atom isotopomers were made in a commercially available White-type borosilicate glass cell (Infrared Analysis Inc., New York) having a base length of 0.82 m and a volume of about 7 l. The spectrometer was fitted with a Si:CaF_2 beamsplitter, CaF_2 cell windows, gold-coated mirrors, an InSb photovoltaic detector, and a tungsten lamp light source with elevated near-IR emission. Optical interference filters having a bandpass appropriate to the measured range were used.

HCN pressures used in the present measurements were in the range of 6.0 to 0.1

mbar, and were measured by two capacitance gauges (MKS baratron). While measuring each spectrum the pressure in the absorption cell was slowly decreasing. The pressure assigned to each spectrum was the average of the initial and final pressure measurement. In some cases the effective average pressure may have been closer to the final pressure measurement. That would account for the transition dipole measurements being too low. The uncertainties in the transition dipoles given in this paper take this slow change into account.

The hydrogen cyanide isotopomers $H^{12}C^{14}N$, $H^{13}C^{14}N$, $H^{12}C^{15}N$, and $H^{13}C^{15}N$ were synthesized by the reaction of equimolar amounts of potassium cyanide with phosphorus pentoxide and an excess of water. The isotopically labeled KCN was commercially available (CIL, Andover, Massachusetts) with a specified isotopic purity of $>99\%$ ^{13}C and $>98\%$ ^{15}N for the monoisotopically substituted samples and 98% $^{13}C^{15}N$ for the doubly substituted sample. In each case the gaseous reaction product was isolated in a cold trap at about 200 K and purified by repeated vacuum distillation. The chemical purity of the different samples was checked both by their vapor pressure and broadband infrared absorption. Only a negligible amount of H_2O and CO_2 could be detected as contamination in the original samples.

The large separation between the DCN and HCN vibrational frequencies and the large difference in the transition dipoles made it easy to observe and measure the spectra of $D^{12}C^{14}N$, $D^{13}C^{14}N$, and $D^{12}C^{15}N$, even though none of the samples was intentionally enriched in deuterium.

The spectra show the strong lines of OCS, CO, and N_2O which were deliberately added in trace quantities for wavenumber calibration or in some cases were outgassed from the absorption cell walls from previous calibration runs. The spectral wavenumbers were calibrated by using the absorption lines of OCS, N_2O, or CO which were present as internal standards in the spectra. The calibration wavenumbers were taken from a recent online update to the calibration book by Maki and Wells (*25*).

APPEARANCE AND ASSIGNMENT OF THE SPECTRA

Figures 1 and 2 show the appearance of the spectra of normal HCN and HCN enriched to about 99% ^{13}C. Both spectra show the two strong HCN bands in the 2100 cm^{-1} region, ν_3 and $3\nu_2$. The spectra also show the closely spaced lines of the OCS band, near 2062 cm^{-1}, which was used for calibration. In Fig. 1, one can see the lines of CO and N_2O which were also useful for calibration. The most important thing to observe in these two spectra is the difference in the relative intensities of the lines in the *R* branch of the ν_3 band. In $H^{12}C^{14}N$ the *R*-branch lines pass through zero intensity at about *R*(7), while in $H^{13}C^{14}N$ the *R* branch seems to be more nearly normal. Actually, the quantitative analysis of the line intensities for $H^{13}CN$ show that the *R*-branch lines pass through zero intensity at *R*(1). In the $H^{13}CN$ spectrum, the intensity maximum in both the *P* and *R* branches is at considerably higher *J*-values than is normal. The appearance of the ν_3 band of $HC^{15}N$ is intermediate between that of HCN and $H^{13}CN$, and the $H^{13}C^{15}N$ lines pass through zero intensity at *P*(1). Figure 3 shows more clearly the variation of the spectral profile with heavy atom isotopic substitution.

Not shown in these figures is the region of the ν_3 band for DCN, which can be seen in the original spectra because the DCN band is over 100 times stronger than the HCN band. It is not the DCN that is unusually strong, but rather it is the HCN band that is unusually weak. Figure 1 was measured with a path length of 96 m and a pressure of about 10 Pa. The relative intensities of the lines in the *P* and *R* branches for the DCN band are also more nearly normal and show very little difference upon substitution with heavy atom isotopes.

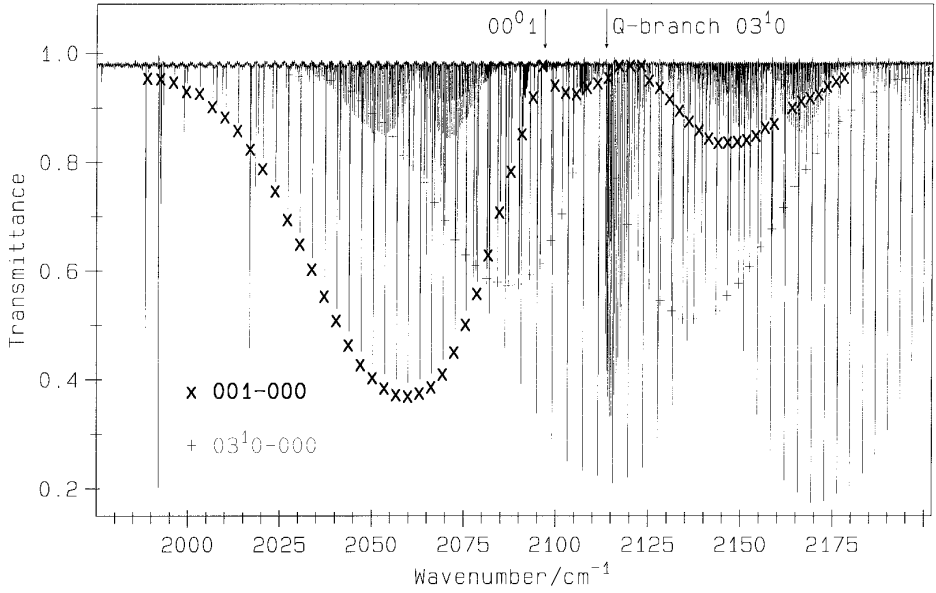

FIG. 1. Spectrum of HCN from 1975 to 2200 cm^{-1}. The lines of the 00^01-00^00 band are indicated by ($\times$) and the lines of the 03^10-00^00 band are indicated by (+). Also present in the spectrum are lines for CO, OCS, and N_2O.

Because the ground state constants are well known for all the isotopic species of HCN studied here, it was possible to verify the assignments of the present work by means of ground state combination-differences. With the exception of the ^{13}C species,

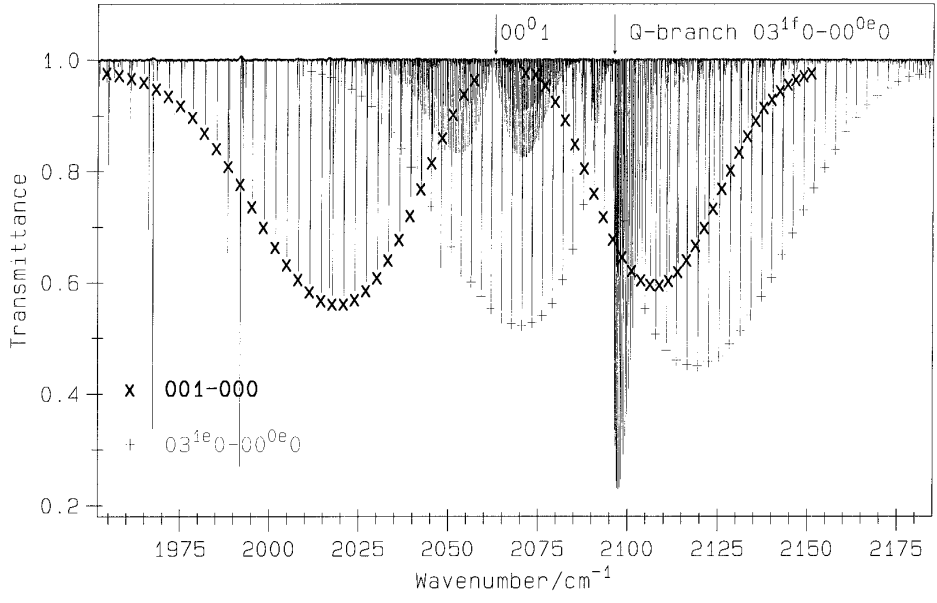

FIG. 2. Spectrum of $H^{13}C^{14}N$ from 1950 to 2185 cm^{-1}. The lines of the 00^01-00^00 band are indicated by ($\times$) and the lines of the 03^10-00^00 band are indicated by (+). The 2062 cm^{-1} band of OCS can also be seen.

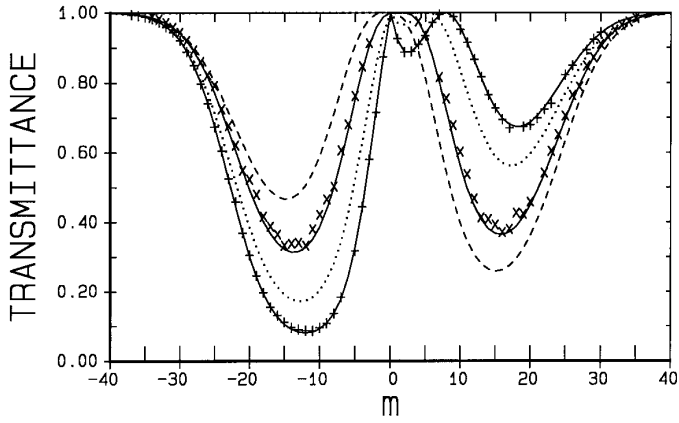

FIG. 3. Comparison of the line intensities for the different isotopomers for a pressure (×) pathlength of about 2.1 cm atm at 298 K. The curves are the calculated values, the dashed line is for $H^{13}C^{15}N$, the dotted line is for $H^{12}C^{15}N$, and the two solid lines are for $H^{12}C^{14}N$ and $H^{13}C^{14}N$. The values given in Table III are indicated by (+) for $H^{12}C^{14}N$ and by (×) for $H^{13}C^{14}N$.

the upper state rotational constants for ν_3 are also well known from microwave studies (*26, 27*) and are in agreement with the present assignments. For the hot bands, 01^11-01^10, combination-differences using the lower state constants from Refs. (*26, 27*) were essential to verify the assignments.

ANALYSIS OF THE MEASUREMENTS

Wavenumbers

For the analysis of the transition wavenumbers we used a least-squares fitting procedure that fit the measurements of several different spectra and also included the fit of the microwave transitions as given by Refs. (*26, 27*) and other references given there. In the fits, the measurements were weighted by the inverse of the square of their estimated uncertainties. The equations used in the fits were

$$E(v, J, l) = G_v + B_v[J(J+1) - l^2] - D_v[J(J+1) - l^2]^2 + H_v[J(J+1) - l^2]^3 \pm \delta_{1,l}\tfrac{1}{2}q_v^0 J(J+1), \quad (1)$$

$$q_v^0 = q_v - q_{vJ}J(J+1) + q_{vJJ}J^2(J+1)^2, \quad (2)$$

and

$$\nu_c = (G_v' - B_v'l'^2) - (G_v'' - B_v''l''^2), \quad (3)$$

which are the same equations that were used by Quapp *et al.* (*3*). Equation (1) uses the Kronecker δ such that $\delta_{1,l} = 1$ only when $l = 1$, otherwise it is zero. With this definition ν_c is the position of the center of the band as observed in the spectrum and the transition wavenumbers are given by

$$\nu_{obs} = E' - E''. \quad (4)$$

Tables I and II give the molecular constants determined from the analysis of the measured line positions. In the present analysis, we have left out of the fit those transitions of the hot band for $H^{12}C^{14}N$ that are most strongly affected by the Coriolis

TABLE I

Rovibrational Constants (in cm^{-1}) for the HCN Bands Measured in This Work

constant	$H^{12}C^{14}N$	$H^{12}C^{15}N$	$H^{13}C^{14}N$	$H^{13}C^{15}N$
00^01-00^00				
ν_c	2096.845 58(3)[a]	2064.316 21(6)	2063.047 34(6)	2029.632 06(5)
B'	1.468 141 99(15)	1.425 579 19(15)	1.430 245 65(51)	1.387 092 87(41)
B''	1.478 221 84(3)	1.435 247 90(10)	1.440 000 56(9)	1.396 431 03(10)
$D'\times10^6$	2.916 09(37)	2.751 24(126)	2.774 93(123)	2.614 85(136)
$D''\times10^6$	2.910 23(22)	2.745 88(109)	2.771 36(85)	2.609 77(119)
$H'\times10^{12}$	3.172(195)	2.363(994)	3.867(761)	3.860(793)
$H''\times10^{12}$	3.265(117)	2.493(827)	5.283(658)	3.973(733)
01^11-01^10				
ν_c	2093.602 08(20)	2061.195 41(10)	2059.338 75(11)	2026.046 02(7)
B'	1.471 573 05(58)	1.428 870 60(43)	1.433 299 44(82)	1.390 013 14(82)
$q'\times10^3$	7.483 008(1009)	7.064 578(491)	7.150 962(1007)	6.736 915(519)
B''	1.481 772 78(11)	1.438 653 05(6)	1.443 157 32(7)	1.399 449 65(16)
$q''\times10^3$	7.487 739 8(21)	7.069 686 3(47)	7.166 164 1(187)	6.749 817 3(235)
$D'\times10^6$	2.982 04(81)	2.812 20(136)	2.836 22(161)	2.671 13(397)
$q_J'\times10^8$	9.086(166)	8.137(78)	7.967(206)	7.243(67)
$D''\times10^6$	2.977 64(28)	2.808 37(117)	2.830 87(89)	2.666 00(403)
$q_J''\times10^8$	8.878 8(27)	8.103 6(78)	8.067 0(95)	7.338 8(124)
$H'\times10^{12}$	[3.941][b]	[3.304]	[6.190]	4.828(1610)
$H''\times10^{12}$	3.998(139)[c]	3.304(993)[d]	6.190(744)	[3.973]

a) The uncertainty in the last digits, twice the standard deviation, is given in parentheses.
b) Values enclosed in square brackets were fixed during the fit.
c) For $H^{12}C^{14}N$ the fit gave $q_{JJ} = 1.420(37)\times10^{-12}$ for the lower level and the same value was used for the upper level.
d) For $H^{12}C^{15}N$ the fit gave $q_{JJ} = 1.474(281)\times10^{-12}$ for the lower level and the same value was used for the upper level.

interaction with the 04^00 level. In forthcoming papers, we shall give the results of the wavenumber analysis of all these bands and many others, including the effects of the Coriolis interactions.

Intensities

The intensity measurements were analyzed in the same way as described in Ref. (*4*). The intensities of individual rovibrational transitions are the measured quantities for this intensity analysis and are given by

$$S_m = p^{-1}l^{-1}\int k(\nu)d\nu, \tag{5}$$

where p is the HCN pressure, l is the absorption pathlength, $k(\nu)$ is the absorption coefficient at wavenumber ν, and the integration is over the entire absorption line. The absorption coefficient is given by $\ln(I_0/I)$. Table III gives the unweighted averages of the measured line intensities, corrected for the isotopic abundance, S_m/C, for the different isotopomers of HCN. Twice as many measurements from two or more spectra were used to determine the constants given in Table IV, but Table III gives a good representation of those measurements. The analysis avoided using lines that had peak absorptions greater than 70% ($k > 1.2$).

The line intensities were determined by applying the INTBAT program developed by Johns (see (*28, 29*)). This program makes a least-squares fit of the line shape to a Voigt profile that has been convolved with the boxcar instrument function. The

TABLE II

Rovibrational Constants (in cm^{-1}) for the DCN Bands Measured in This Work

constant	$D^{12}C^{14}N$	$D^{12}C^{15}N$	$D^{13}C^{14}N$	$D^{13}C^{15}N$
00^01-00^00				
ν_c	1925.255 56(37)[a]	1900.100 45(4)	1911.841 53(5)	1885.322 91(7)
B'	1.201 206 74(28)	1.166 849 55(14)	1.180 668 18(49)	1.145 684 61(16)
B''	1.207 750 95(3)	1.173 138 247(3)	1.187 076 29(9)	1.151 840 26(12)
$D'\times10^6$	1.925 72(89)	1.812 33(52)	1.856 97(82)	1.741 59(185)
$D''\times10^6$	1.927 10(53)	1.816 20(50)	1.856 52(115)	1.744 04(201)
$H'\times10^{12}$	[2.82][b]		[2.83]	
$H''\times10^{12}$	2.82(29)	[2.8]	2.85(89)	
01^11-01^10				
ν_c	1928.094 85(42)	1903.023 73(70)	1913.813 94(330)	
B'	1.205 317 0(36)	1.170 833 2(76)	1.184 468 8(630)	
$q'\times10^3$	6.391 14(432)	6.019 3(91)	6.285 3(183)	
B''	1.212 072 64(8)	1.177 306 36(6)	1.191 059 26(7)	
$q''\times10^3$	6.210 659 43(171)	5.873 430 8(33)	6.080 683(28)	
$D'\times10^6$	1.992 60(682)	1.882 6(141)	2.062(231)	
$q_J'\times10^8$	7.19(106)	5.91(220)	[6.93]	
$D''\times10^6$	1.997 01(55)	1.881 69(70)	1.920 01(111)	
$q_J''\times10^8$	7.347 5(22)	6.714 9(57)	6.930 6(178)	
$H'\times10^{12}$	[3.66]		[3.9]	
$H''\times10^{12}$	3.66(29)[c]	4.11(46)[d]	3.92(83)[e]	

a) The uncertainty in the last digits, twice the standard deviation, is given in parentheses.
b) Values enclosed in square brackets were fixed during the fit.
c) For $D^{12}C^{14}N$ the fit gave $q_{JJ} = 1.458(25)\times10^{-12}$ for the 01^10 level and the same value was used for the 01^11 level.
d) For $D^{12}C^{15}N$ the fit gave $q_{JJ} = 1.194(198)\times10^{-12}$ for the 01^10 level and the same value was used for the 01^11 level.
e) For $D^{13}C^{14}N$ the fit gave $q_{JJ} = 1.297(211)\times10^{-12}$ for the 01^10 level and the same value was used for the 01^11 level.

program has the capability of determining a pressure broadening parameter but, for those spectra with small pressure broadening, the pressure broadening was fixed at values given by Pine (*30*). For DCN, we have no good estimate for the pressure broadening and the uncertainty in that parameter makes the DCN intensity measurements a little less reliable. For a given point the difference between the measurement and the fitted line shape is usually less than 0.5%.

The transition dipole, $|R_v|$, is related to the line intensity, S_m, by the equation

$$|R_v|^2F = (S_m 3hcQ_rQ_vT)/8\pi^3\nu_m L_m 273.15\mathcal{L}C \exp[-E''/kT](1 - \exp[-\nu_m/kT]), \quad (6)$$

where Q_r and Q_v are the rotational and vibrational partition functions, $\mathcal{L}$ is Loschmidt's number, E'' is the energy of the lower state rovibrational level, T is the temperature, L_m is the Hönl–London factor, F is the Herman–Wallis term, C is the isotopic abundance of the species being considered, and ν_m is the wavenumber of the line. For this work we used Q_v = {1.0676, 1.1143} for {HCN, DCN} and Q_r = {140.45, 140.11, 171.82, 171.20} for the states {HCN 000, HCN 010, DCN 000, DCN 010}, respectively, at 298 K. All of the terms on the right-hand side of Eq. (6) are known or measured in this work.

The values for the vibrational transition dipoles are given in Table IV along with the Herman–Wallis constants needed to fit the measured intensities. As in our earlier paper (*4*), we have adopted the expression

$$F = \{1 + A_1m + A_2m^2\}^2 \quad (7)$$

TABLE III

Averages of the Measured Line Intensities, S_m/C, (in cm^{-2} atm^{-1} at 298 K) for the 00^01-00^00 Band of Different Isotopomers of HCN

P-BRANCH						*R*-BRANCH				
$H^{12}C^{14}N$	$H^{12}C^{15}N$	$H^{13}C^{14}N$	$H^{13}C^{15}N$	$D^{12}C^{14}N$	J''	$H^{12}C^{14}N$	$H^{12}C^{15}N$	$H^{13}C^{14}N$	$H^{13}C^{15}N$	$D^{12}C^{14}N$
					0	1.93E-4	1.11E-4		1.09E-5	7.47E-4
3.37E-4				8.49E-4	1	3.00E-4	7.69E-5		5.19E-5	1.56E-3
8.39E-4	3.90E-4			1.54E-3	2	2.95E-4	6.36E-5			2.17E-3
1.36E-3	7.48E-4	2.26E-4	5.02E-5	2.30E-3	3	2.36E-4		6.30E-5	3.10E-4	2.76E-3
2.03E-3		4.16E-4		3.05E-3	4	1.71E-4		1.67E-4	5.34E-4	2.97E-3
2.87E-3	1.67E-3	6.79E-4	2.47E-4	3.50E-3	5	7.25E-5			8.32E-4	3.37E-3
	2.14E-3	9.59E-4	4.25E-4	3.87E-3	6	1.61E-5		5.10E-4		3.74E-3
4.23E-3	2.67E-3	1.25E-3	6.39E-4	4.35E-3	7		1.58E-4	7.03E-4	1.58E-3	3.94E-3
4.97E-3	3.05E-3	1.72E-3	9.18E-4	4.58E-3	8	2.97E-5	2.93E-4	9.73E-4		
5.55E-3	3.40E-3	1.91E-3	1.12E-3	4.79E-3	9	1.24E-4	4.47E-4	1.27E-3		3.97E-3
5.86E-3	3.79E-3	2.16E-3	1.36E-3	4.65E-3	10	2.22E-4	6.53E-4	1.55E-3		3.83E-3
6.11E-3	4.17E-3	2.42E-3	1.56E-3		11	3.58E-4	8.58E-4	1.90E-3		3.64E-3
6.09E-3	4.37E-3	2.75E-3	1.73E-3		12	5.06E-4	1.04E-3	2.21E-3		3.35E-3
6.00E-3	4.41E-3	2.69E-3			13	6.70E-4	1.06E-3	2.24E-3		3.07E-3
5.84E-3	4.32E-3	2.71E-3	1.91E-3		14	7.96E-4	1.17E-3	2.34E-3	3.40E-3	
5.46E-3	4.11E-3	2.75E-3	1.92E-3		15	9.10E-4	1.39E-3	2.48E-3		2.40E-3
5.08E-3	3.86E-3	2.52E-3	1.88E-3		16	1.00E-3	1.29E-3	2.42E-3		2.10E-3
4.66E-3	3.57E-3	2.37E-3			17		1.29E-3	2.13E-3		1.83E-3
4.06E-3	3.18E-3	2.19E-3	1.65E-3		18	9.88E-4	1.38E-3	2.15E-3	2.93E-3	1.49E-3
3.51E-3	2.64E-3	1.84E-3	1.50E-3		19	9.67E-4	1.33E-3	1.95E-3		1.26E-3
2.97E-3	2.32E-3	1.62E-3	1.33E-3		20	8.95E-4				1.03E-3
2.49E-3	2.00E-3	1.50E-3	1.17E-3		21	8.07E-4	1.06E-3	1.53E-3		8.17E-4
1.95E-3	1.69E-3	1.19E-3	9.94E-4		22	7.52E-4	9.27E-4	1.26E-3		6.56E-4
1.61E-3	1.37E-3	9.74E-4	8.34E-4		23		7.73E-4	1.07E-3		5.01E-4
1.26E-3	1.07E-3	8.05E-4	6.89E-4		24	4.90E-4	6.51E-4	8.73E-4		3.92E-4
9.89E-4	8.60E-4	5.85E-4	5.51E-4		25	4.09E-4	5.04E-4	6.72E-4	9.07E-4	3.03E-4
7.51E-4	6.46E-4	4.92E-4	4.42E-4		26		4.28E-4	5.96E-4	7.18E-4	
5.70E-4	4.86E-4	3.78E-4	3.44E-4		27	2.81E-4	3.41E-4	4.13E-4	5.59E-4	2.16E-4
4.06E-4	3.81E-4	2.83E-4	2.64E-4		28	1.99E-4	2.47E-4	3.45E-4	4.31E-4	1.32E-4
2.97E-4	2.52E-4	2.10E-4	1.97E-4		29	1.45E-4	2.07E-4	2.37E-4	3.15E-4	
2.07E-4	1.87E-4	1.47E-4	1.46E-4		30		1.45E-4	1.78E-4	2.36E-4	
1.44E-4	1.32E-4	1.08E-4	1.04E-4		31		1.09E-4	1.29E-4	1.70E-4	
1.05E-4	8.99E-5	7.26E-5	7.56E-5		32		8.57E-5	9.03E-5	1.24E-4	
6.63E-5	6.27E-5	4.95E-5	5.00E-5		33			6.51E-5	8.67E-5	
4.40E-5	3.99E-5	3.26E-5	3.33E-5		34			4.10E-5	5.75E-5	
2.91E-5	2.61E-5		2.49E-5		35				4.25E-5	
2.00E-5	1.67E-5				36				2.80E-5	
1.48E-5	1.05E-5				37					
					38					
	4.13E-6				39					

Note. The uncertainties are about 5 percent of the values.

for the Herman–Wallis term for the *P*- and *R*-branch transitions. In the present work, no intensities were measured for any *Q*-branch transitions. Here m has the usual value, $m = \Delta J(J' + J'' + 1)/2$. Since F is given as the square of a real function, it can never assume negative values, although it can go through zero at some value of m or J. Normally the value of the A_1 constant is on the order of ± 0.01 or less (*4*) and that of the A_2 constant is on the order of ± 0.001 or less. In the next section, we show that the large values found for A_1 for the CN stretching vibration of different isotopomers of HCN is a natural consequence of the small transition dipole and the large permanent dipole moment.

One of the difficulties of making low-pressure intensity measurements is being certain that the measured pressure is truly the pressure of the compound of interest. Even if the sample is free of contamination, the absorption cell usually is not and for long path absorption cells a small amount of an adsorbed gas can be displaced from the surfaces exposed to the sample gas. For relative intensity measurements the FTS technique has the advantage that for a given spectrum all lines are measured at the same time, or at least over the same period of time. Even if the partial pressure of

TABLE IV

Measured Transition Dipole and Herman–Wallis Constants

molecule	R_v(observed) debye[a]	R_v(calc) debye	A_1	$A_2\times10^3$	$R_vA_1\times10^3$(obs) debye	$R_vA_1\times10^3$(calc) debye
00^01-00^00						
$H^{12}C^{14}N$	0.001 362(4)[b]{12}[c]	0.00142	-0.1254(2)	-0.25(1)	-0.171	-0.178
$H^{12}C^{15}N$	0.000 900(3){40}	0.00095	-0.1829(6)	-0.38(1)	-0.165	-0.174
$H^{13}C^{14}N$	0.000 309(2){18}	0.00032	-0.539(3)	-1.11(2)	-0.166	-0.172
$H^{13}C^{15}N$	-0.000 130(2){4}	-0.000134	1.25(2)	2.40(6)	-0.163	-0.167
$D^{12}C^{14}N$	0.022 74(8){60}	0.0254	-0.0076(2)		-0.173	-0.193
$D^{12}C^{15}N$	0.023 1(1){15}	0.0247	-0.0076(3)		-0.176	-0.188
$D^{13}C^{14}N$		0.0232	-0.0081(1)	0.003(15)		-0.188
01^11-01^10						
$H^{12}C^{14}N$	-0.001 794(3){16}	-0.00187	0.0954(1)	0.25(1)	-0.171	-0.178
$H^{12}C^{15}N$	-0.002 52(6){10}	-0.00255	0.068(5)	0.17(14)	-0.170	-0.174
$H^{13}C^{14}N$	-0.002 63(3){16}	-0.00282	0.061(2)	0.16(9)	-0.161	-0.172
$H^{13}C^{15}N$	-0.003 22(1){10}	-0.00328	0.0510(3)	0.06(3)	-0.164	-0.167
$D^{12}C^{14}N$	0.023 0(4){6}	0.0214	-0.009(2)	-0.3(1)	-0.21	-0.193
$D^{12}C^{15}N$	0.022 5(2){15}	0.0235	-0.0080(8)		-0.18	-0.188
10^00-00^00						
$H^{12}C^{14}N$	0.083 1(17)[d]	0.0846	-0.00149(5)[d]	-0.012(3)	-0.124	-0.126
$D^{12}C^{14}N$	0.062 0(1){18}	0.0563	-0.00102(4)	0.009(3)	-0.063	-0.057

a) 1 debye = $3.335\,64\times10^{-30}$ Cm.

b) The uncertainty, one standard deviation, in the last digits as given by the least-squares fit is given in parentheses.

c) The curly brackets, {}, indicate the range of uncertainty in the last digits due to the uncertainty in the partial pressure measurement.

d) The transition dipole comes from the intensity given in Ref. (*31*). The Herman-Wallis constants come from a fit for $H^{12}C^{15}N$.

the gas was changing during the course of measuring a single spectrum, which takes several hours, the effective partial pressure of a given molecular species is the same for all lines in the spectrum. For HCN, the same can be said for all isotopomers because they all will show nearly the same behavior with respect to adsorption and desorption from the cell walls.

In addition to measurements on isotopically enriched samples of $H^{13}C^{14}N$, $H^{12}C^{15}N$, and $H^{13}C^{15}N$, we have tried to estimate the intensity of DCN and other deuterated isotopomers without intentionally adding deuterium to the sample. Normally the D/H ratio is about 0.000148, but in a laboratory that makes many measurements on deuterium enriched samples, the possibility of contamination is quite high. Hydrogen is quite labile in HCN and will quickly exchange with deuterium in any equally labile compound such as HDO.

The effect of such contamination was quite evident from a comparison of the intensity of ν_3 of DCN observed in two spectra of normal HCN, one spectrum at high pressure, 490 Pa, and one at low pressure, 31 Pa. The intensities, S_m, of the DCN lines in the low-pressure spectrum were twice those measured in the high-pressure spectrum. We report in Table IV the transition dipole determined from the high-pressure measurement but expect that it might be too high if there is any unexpected deuterium contamination. Comparison with earlier measurements indicate that is not the case.

Based on the transition dipoles given in Table IV for normal HCN and DCN, we were able to estimate the deuterium enrichment in one spectrum of $HC^{15}N$. In the spectrum of $HC^{15}N$, it was possible to measure a few lines of $D^{12}C^{14}N$ relative to

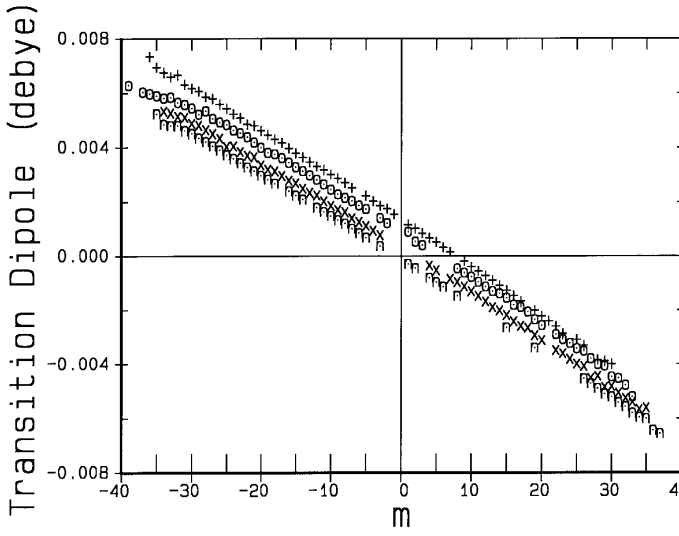

FIG. 4. Plot of the effective transition dipole, given by the square-root of the left side of Eq. (6) vs the rotational quantum number m. The transition dipoles have been given signs that agree with the signs in Table IV for $m = 0$. Note that all isotopomers have nearly the same slope at the $m = 0$ crossing point. The symbols are as follows: (+) for $H^{12}C^{14}N$, (0) for $H^{12}C^{15}N$, (×) for $H^{13}C^{14}N$, and (n) for $H^{13}C^{15}N$.

$H^{12}C^{14}N$ in order to determine the D/H ratio in that sample and it was found to be enriched by a factor of 4.09 ± 0.2 over what was observed in the normal HCN spectrum. This leaves a rather large uncertainty in the ν_3 intensity for $D^{12}C^{15}N$.

Since the lines of $D^{12}C^{14}N$ were too weak to measure in the spectrum enriched in ^{13}C, it was not possible to measure the deuterium concentration and therefore the transition dipole for ν_3 of $D^{13}CN$, even though we have a very good measurement of the Herman–Wallis constant A_1. We also have no good measurement of the transition dipole for $D^{13}C^{15}N$.

CALCULATION OF THE TRANSITION DIPOLE FROM THE HERMAN–WALLIS CONSTANT

In Fig. 4, we show plots of the square-root of the left-hand side of Eq. (6) vs rotational quantum number, m, for the different isotopomers of HCN. Even though the different isotopomers have quite different values for the vibrational transition dipole, R_3, and the dominant Herman–Wallis constant, A_1, the curves are nearly parallel. This means that the slope, given by $R_3 \times A_1$, must be nearly constant for all isotopomers. These plots do not provide any information on the sign of the transition dipole, but the sign of the Herman–Wallis constant does come from the zero-intensity intercept of $|R_v|^2F$ vs m.

Watson (*2*) has derived the relationship between μ_3 and A_1 for linear molecules. Watson has also given references to earlier papers that treat the Herman–Wallis constants for linear molecules. Combining Eqs. (54), (30), and (28) of Watson's paper and noting the difference between his μ_v and our R_v, we have

$$A_1(\text{for } \nu_3) = 2^{-1/2}[-4B(\omega_3\omega_2)^{1/2}(\omega_3^2 - \omega_2^2)^{-1}\zeta_{23}R_2/R_3 - 2(2B/\omega_3)^{3/2}\zeta_{12}\mu_e/R_3] \quad (8)$$

and

$$A_1(\text{for } \nu_1) = 2^{-1/2}[4B(\omega_1\omega_2)^{1/2}(\omega_1^2 - \omega_2^2)^{-1}\zeta_{12}R_2/R_1 - 2(2B/\omega_1)^{3/2}\zeta_{23}\mu_e/R_1]. \quad (9)$$

TABLE V

Constants[a] Used in the Calculation of the Transition Dipole

molecule	ω_1 cm^{-1}	ω_2 cm^{-1}	ω_3 cm^{-1}	ζ_{12}	ζ_{23}	B_0 cm^{-1}	μ_0 debye	R_1 debye	R_2 debye
$H^{12}C^{14}N$	3441.16	727.10	2128.67	0.9882	0.1529	1.47822	2.985	0.0831	-0.190
$H^{12}C^{15}N$	3439.85	726.01	2095.12	0.9881	0.1536	1.43525	2.985	0.0831	-0.190
$H^{13}C^{14}N$	3422.04	720.71	2094.16	0.9866	0.1631	1.44000	2.985	0.0831	-0.190
$H^{13}C^{15}N$	3420.	719.	2065.	0.9865	0.1638	1.39643	2.985	0.0831	-0.190
$D^{12}C^{14}N$	2703.34	579.85	1952.12	0.9962	-0.0871	1.20775	2.9908	0.0620	-0.11
$D^{12}C^{15}N$	2694.30	578.49	1925.83	0.9974	-0.0719	1.17314	2.9908	0.0620	-0.11
$D^{13}C^{14}N$	2661.58	571.82	1938.52	0.9979	-0.0645	1.18708	2.9908	0.0620	-0.11

a) The constants in the first five columns of numbers were taken from Ref. (*34*). The constants in the last column were taken from Refs. (*4*) and (*5*).

For heavy atom substitutions, the terms on the right-hand side of Eqs. (8) and (9) are nearly constant, with the exception of R_3. Consequently, Eq. (8) shows that the product $R_3 \times A_1$ is hardly affected by heavy atom substitutions. This is also shown by the last column of Table IV.

Watson has also given a correction term that must be added to Eqs. (8) and (9) when $\pi - \pi$ transitions are concerned, such as the hot bands, 01^11-01^10. In this paper, we have left out that correction term because it is small compared to the other terms and includes higher order terms that we could not evaluate with confidence.

For the present measurements, the Herman–Wallis constant can be determined with more accuracy than the transition dipole. Consequently, we have used Eq. (8) to calculate the transition dipole, R_3, from the observed Herman–Wallis constant, A_1(for ν_3), for the different isotopomers of HCN. The constants used in the calculation as well as the calculated and observed values for the transition dipoles are given in Tables IV and V. To within experimental error, the calculated values for the transition dipole are in agreement with the measured values. It is particularly gratifying that we can even calculate the transition dipole for DCN with similar accuracy even though the Herman–Wallis effect is much smaller and therefore might be subject to higher order effects as well as being less accurate.

We have also used Eq. (9) to calculate the transition dipoles, R_1, from the corresponding Herman–Wallis constants, A_1 (for ν_1). For HCN, we used the measurements of Smith *et al.* (*31*) of the intensity for the C—H stretching fundamental, ν_1 in our notation. Because of the limited resolution available to them, the uncertainty in their Herman–Wallis constant is too large to provide a quantitative check of Eq. (9). In one of our spectra we were able to measure the Herman–Wallis constants for ν_1 of $H^{12}C^{15}N$ and used those values for the next to last line of Table IV in the expectation that the Herman–Wallis constant for ν_1 will be nearly the same for $H^{12}C^{14}N$ and $H^{12}C^{15}N$.

In addition, the spectrum that gave the best measurements for the ν_3 band of DCN extended to above the ν_1 band and gave a good measurement for the intensity of ν_1 and the Herman–Wallis constant as given in Table IV. It is not clear if the disagreement with Eq. (9) is due to errors in the numbers used in the calculation, or is what should be expected from the application of Eq. (9) to a real spectrum. We have no past experience in comparing the Herman–Wallis constants calculated with Eq. (9) to the constants obtained from a real spectrum.

In this work we have ignored the possibility that the nearby $3\nu_2$ band may be affecting the intensity of the CN stretch through a Coriolis interaction. Since the

matrix element for such an interaction is J-dependent, it will make a direct contribution to the A_1 Herman–Wallis constant. Because of the large difference in the B_v values for the interacting levels, there should also be a contribution to the higher order Herman–Wallis constants. The effect of that interaction would be quite different for different isotopomers because the separation of the interacting levels is 17, 33, 46, and 230 cm^{-1} for $H^{12}C^{14}N$, $H^{13}C^{14}N$, $H^{12}C^{15}N$, and $D^{12}C^{14}N$, respectively. It would be quite unlikely to have a significant effect on the DCN measurements. However, it may contribute to the discrepancies between the observed and calculated transition dipoles for ν_3 of HCN. The intensity and Herman–Wallis constants have been determined for $3\nu_2$ of $H^{12}C^{14}N$ (*4*) and seem quite normal.

A related Coriolis interaction has been detected between the $01^{1e}1$ and $04^{0}0$ vibrational states (*20, 32*) which will affect the intensities of some of the $01^{1e}1–01^{1e}0$ transitions for $H^{12}C^{14}N$, especially near the point where the two levels cross, $J = 10$. That interaction does not affect the intensities of the $01^{1f}1–01^{1f}0$ transitions and the interaction is also very weak for the other isotopomers. Only in the case of $H^{12}C^{14}N$ is there a crossing of the interacting levels and therefore, only in that case is the mixing of the interacting levels large enough to have an unmistakable effect on the intensities. We believe we have excluded from the analysis all levels that have a significant intensity perturbation due to this Coriolis interaction.

In this analysis we have not attempted to understand the values found for the second Herman–Wallis constant, A_2. These constants may be affected by the Coriolis interaction between ν_3 and $3\nu_2$ but it seems more likely that they are related to the values of A_1. For ν_3 the ratio A_1/A_2 is 500 ± 20 for all isotopomers of HCN. Because A_1 changes by a factor of 10 and even changes sign, it is unlikely that this constant ratio is accidental.

DISCUSSION

The transition dipoles measured for ν_1 and ν_3 of DCN can be compared with earlier measurements. The band intensity measurements of Hyde and Hornig (*5*) are equivalent to the transition moments $|R_1| = 0.0679 \pm 0.0012$ and $|R_3| = 0.0239 \pm 0.0004$ D and those of Kim and King (*8*) are equivalent to $|R_1| = 0.0641 \pm 0.0005$ and $|R_3| = 0.0248 \pm 0.0004$ D. Those values are larger than the present results, which is surprising because we believe our results represent an upper limit. This may indicate that our effective partial pressure should be lower than we thought. This would also explain the consistent difference between the observed and calculated transition dipoles as given in Table IV.

Our measurements of R_1 and R_3 of DCN came from the same spectrum, consequently the accuracy of the ratio $|R_1|/|R_3| = 2.726 \pm 0.020$ should be correctly given by the least-squares fits, regardless of the accuracy of the partial pressure measurement. That ratio is in very good agreement with the ratios given by the earlier measurements, 2.841 and 2.585, respectively.

The present measurements give an integrated band intensity of 0.115 cm^{-2} atm^{-1} at 298 K for the CN stretching fundamental of $H^{12}C^{14}N$. This value is very close to the estimate made by Smith *et al.* of ca. 0.1 cm^{-2} atm^{-1} (*33*). Hyde and Hornig (*5*) found a much larger value (0.59 cm^{-2} atm^{-1} at 298 K) from their low-resolution measurements at much higher pressures where they were subject to interference from absorption by the dimer $(HCN)_2$.

As shown in Table IV, the present measurements of the transition dipoles are consistently lower than the values calculated using Eq. (8). The disagreement between

the observed and calculated transition dipoles might be explained by the errors in the measurements of the transition dipoles (possibly due to errors in the partial pressure determination). In most cases the discrepancy would disappear if the true value of the transition dipole were near the high end of the uncertainties given in Table IV.

In our calculations we have used the values of B_0 and μ_0 instead of the equilibrium values, but that does not change the results significantly. We have also tried using the observed band centers instead of the harmonic frequencies without obtaining any better agreement. Perhaps the Coriolis zeta constants are less accurate than expected from the uncertainties given by Nakagawa and Morino (*34*). Although there have been a number of more recent papers that analyze the potential constants of HCN, none of them has published values for the zeta constants of so many isotopomers. More recent values have been given for the harmonic frequencies but they do not change the calculated transition dipoles by a significant amount.

The present measurements provide information on the relative signs of the transition dipoles. Tables IV and V give what seem to be the only signs for the transition dipoles that are consistent with Eqs. (8) and (9), with the measured Herman–Wallis constants, with the signs given for the zeta constants by Nakagawa and Morino, and with a positive value for the HCN dipole moment. Of particular interest is the sign reversal observed in the ν_3 transition dipole, R_3, in going from $H^{13}C^{14}N$ to $H^{13}C^{15}N$. This is shown by the change in sign of the Herman–Wallis constant, A_1. There is a clear trend in the magnitude and sign of R_3 in going from DCN, where the isotopic substitution is on the CH (or CD) part of the molecule, to $H^{13}C^{15}N$, where the substitutions are on the CN part of the molecule.

The ν_1 transition dipole, R_1, has the same sign for all isotopomers. This is to be expected because the transition dipole for the CH stretching fundamental has parallel, rather than opposing contributions from both the CH and CN stretching motions that go into the CH normal mode.

For ν_3, a sign reversal is also observed in going from the ground state transitions to the hot-band transitions for most HCN isotopomers. This effect is just a normal change of about 0.003 D in the transition dipole with change in vibrational state ($0.00136 - 0.00315 = -0.00179$ D). Aside from this displacement to more negative values for the hot-band transition dipoles, the trend with isotopic substitution is the same as observed for the ground state transition dipoles.

We have shown that the transition dipole for the CN stretching vibration is so small that it is very sensitive to heavy atom substitutions and even passes from positive to negative when ^{15}N is substituted for ^{14}N in $H^{13}CN$. We have also shown that, within the accuracy of the various constants used in the calculation, Eq. (8) gives the correct relationship between the Herman–Wallis constant and the transition dipole.

The large Herman–Wallis constant and the small transition dipole result in almost the entire intensity of the CN stretching fundamental bands for $H^{13}C^{14}N$ and $H^{13}C^{15}N$ being borrowed from the pure dipole moment. The band intensity given by summing the intensities of all the rovibrational transitions in the $H^{13}C^{15}N$ band is 0.079 cm^{-2} atm^{-1}, while the sum of the line intensities calculated from the transition dipole without the Herman–Wallis terms would be 0.00033 cm^{-2} atm^{-1} or 200 times smaller. Since the Coriolis derived intensity increases with increasing J, the intensity maxima in both the P and R branches for $H^{13}C^{14}N$ and $H^{13}C^{15}N$ are shifted to much higher J-values than one would expect for a normal band, $J'' = 15$ vs $J'' = 8$ observed for ν_1 of HCN.

ACKNOWLEDGMENTS

The authors A.M. and W.Q. thank Brenda and Manfred Winnewisser for their continued interest in this work and for their hospitality during visits to Giessen. We also thank John Johns (of the NRC of Canada)

for allowing us to use the line-fitting program that he and others developed for the analysis of Fourier transform spectra. We thank J. K. G. Watson for discussions relating to the application of Eqs. (8) and (9) to the present measurements; however, we are solely responsible for any errors in the interpretation of these measurements. This project was possible with financial support from the Deutsche Forschungsgemeinschaft.

REFERENCES

1. N. Jacobi and J. H. Jaffe, *J. Mol. Spectrosc.* **10,** 1–11 (1963).
2. J. K. G. Watson, *J. Mol. Spectrosc.* **125,** 428–441 (1987).
3. W. Quapp, S. Klee, G. Ch. Mellau, S. Albert, and A. G. Maki, *J. Mol. Spectrosc.* **167,** 375–382 (1994).
4. A. G. Maki, W. Quapp, and S. Klee, *J. Mol. Spectrosc.* **171,** 420–434 (1995).
5. G. E. Hyde and D. F. Hornig, *J. Chem. Phys.* **20,** 647–652 (1952).
6. R. E. Bruns and W. B. Pearson, *J. Chem. Phys.* **53,** 1413–1417 (1970).
7. R. E. Bruns and B. B. Neto, *J. Chem. Phys.* **68,** 847–851 (1978).
8. K. Kim and W. T. King, *J. Chem. Phys.* **71,** 1967–1972 (1979).
9. R. Herman and R. F. Wallis, *J. Chem. Phys.* **23,** 637–646 (1955).
10. R. Herman and R. J. Rubin, *Astrophys. J.* **121,** 533–540 (1955).
11. R. Herman, R. W. Rothery, and R. J. Rubin, *J. Mol. Spectrosc.* **2,** 369–386 (1958); *J. Mol. Spectrosc.* **9,** 170–171 (1962).
12. N. Jacobi, *J. Mol. Spectrosc.* **22,** 76–79 (1967).
13. R. H. Tipping and R. M. Herman, *J. Mol. Spectrosc.* **36,** 404–414 (1962).
14. M. T. Emerson and D. F. Eggers, *J. Chem. Phys.* **37,** 251–259 (1962).
15. M. R. Aliev, *Opt. Spektrosk.* **60,** 1081–1083 (1986); *Opt. Spectrosc. (English Transl.)* **60,** 669–670 (1986).
16. M. R. Aliev and J. K. G. Watson, *in* ''Molecular Spectroscopy: Modern Research,'' Vol. III, pp. 1–67, Academic Press, New York, 1985.
17. J. K. G. Watson, *J. Mol. Spectrosc.* **132,** 477–482 (1988).
18. Ph. Arcas, E. Arié, Ph. Cardinet, A. Valentin, and A. Henry, *J. Mol. Spectrosc.* **81,** 262–268 (1980).
19. Ph. Arcas, E. Arié, A. Valentin, and A. Henry, *J. Mol. Spectrosc.* **96,** 288–293 (1982).
20. A. G. Maki and D. R. Lide, *J. Chem. Phys.* **47,** 3206–3210 (1967).
21. A. G. Maki and R. L. Sams, *J. Mol. Spectrosc.* **60,** 57–62 (1976).
22. J.-I. Choe, D. K. Kwak, and S. G. Kukolich, *J. Mol. Spectrosc.* **121,** 75–83 (1987).
23. J. Bentsen and H. G. M. Edwards, *J. Raman Spectrosc.* **2,** 407–421 (1974).
24. K. A. Keppler, Thesis, The Ohio State University, Columbus, OH, 1994.
25. A. G. Maki and J. S. Wells, ''Wavenumber Calibration Tables from Heterodyne Frequency Measurements,'' NIST Special Publication 821, U.S. Government Printing Office, Washington, DC, 1991; also available in updated form over the World Wide Web with a Mosaic-like browser at HTTP://physics.nist.gov/
26. F. C. De Lucia and P. A. Helminger, *J. Chem. Phys.* **67,** 4262–4267 (1977).
27. J. Preusser and A. G. Maki, *J. Mol. Spectrosc.* **162,** 484–497 (1993).
28. J. W. C. Johns and J. Van der Auwera, *J. Mol. Spectrosc.* **140,** 71–102 (1990).
29. J. W. C. Johns, *J. Mol. Spectrosc.* **125,** 442–464 (1987).
30. A. S. Pine, *J. Quant. Spectrosc. Radiat. Transfer* **50,** 149–166 (1993).
31. M. A. H. Smith, G. A. Harvey, G. L. Pellet, A. Goldman, and D. J. Richardson, *J. Mol. Spectrosc.* **105,** 105–112 (1984).
32. A. G. Maki, W. B. Olson, and R. L. Sams, *J. Mol. Spectrosc.* **36,** 433–447 (1970).
33. I. W. M. Smith, *J. Chem. Soc. Faraday Trans. 2* **77,** 2357–2363 (1981).
34. T. Nakagawa and Y. Morino, *Bull. Chem. Soc. Jpn.* **42,** 2212–2219 (1969).